JOURNAL OF GEOPHYSICAL RESEARCH, VOL. 99, NO. D10, PAGES 21,005–21,016, OCTOBER 20, 1994

Comparison of upper tropospheric water vapor from GOES, Raman lidar, and cross-chain loran atmospheric sounding system measurements

B. J. Soden[1,2], S. A. Ackerman[3], D. O'C. Starr[4], S. H. Melfi[4], and R. A. Ferrare[5]

Abstract. Observations of upper tropospheric relative humidity obtained from Raman lidar and CLASS sonde instruments obtained during the FIRE Cirrus-II field program are compared with satellite measurements from the GOES 6.7-μm channel. The 6.7-μm channel is sensitive to water vapor integrated over a broad layer in the upper troposphere (roughly 500-200 mbar). Instantaneous measurements of the upper tropospheric relative humidity from GOES are shown to agree to within roughly 6% of the nearest lidar observations and 9% of the nearest CLASS observations. The CLASS data exhibit a slight yet systematic dry bias in upper tropospheric humidity, a result which is consistent with previous radiosonde intercomparisons. Temporal stratification of the CLASS data indicates that the magnitude of the bias is dependent upon the time of day, suggesting a solar heating effect in the radiosonde sensor. Using CLASS profiles, the impact of vertical variability in relative humidity upon the GOES upper tropospheric humidity measurements is also examined. The upper tropospheric humidity inferred from the GOES 6.7-μm channel is demonstrated to agree to within roughly 5% of the relative humidity vertically averaged over the depth of atmosphere to which the 6.7-μm channel is sensitive. The results of this study encourage the use of satellite measurements in the 6.7-μm channel to quantitatively describe the distribution and temporal evolution of the upper tropospheric humidity field.

1. Introduction

Clouds form in moist environments. The First ISCCP Regional Experiment (FIRE) Cirrus-II Implementation Plan (August, 1990) noted the need for mesoscale measurements of upper tropospheric water vapor content. These measurements are required for initializing and verifying numerical weather prediction models, for describing the environments in which cirrus clouds develop and dissipate, and for understanding the role of upper tropospheric water vapor on the radiative energy balance [*Starr and Melfi*, 1991]. The need for accurate upper tropospheric water vapor measurements has been further emphasized by systematic discrepancies noted between different radiosonde sensors [*Garand et al.*, 1992; *Schmidlin*, 1989] and by spurious trends in radiosonde measurements of relative humidity in the upper troposphere [*Elliot and Gaffen*, 1991]. FIRE Cirrus-II took place over Coffeyville Kansas from November 12 to December 7, 1991. During this time, a variety of instruments were deployed to measure the water vapor amounts in the upper troposphere including Raman lidar and Cross-chain Loran Atmospheric Sounding System (CLASS) sondes.

The formation, maintenance, and dissipation of cirrus clouds involve the time variations of the water budget of the upper troposphere. The GOES 6.7-μm radiance observations are sensitive to the upper tropospheric relative humidity in a broad layer extending from roughly 500 to 200 mbar (see Figure 1). High 6.7-μm brightness temperatures indicate a relatively dry upper troposphere and are associated with regions generally free of cirrus clouds. Brightness temperatures that are lower, implying higher relative humidity, may or may not have cirrus present. Animation of time sequences of 6.7-μm images was particularly useful in describing the upper tropospheric synoptic conditions for planning various FIRE Cirrus-II missions. The 6.7-μm observations have also been shown to be valuable for describing the climatology of upper tropospheric water vapor [*Van de Berg et al.*, 1991; *Soden and Bretherton*, 1993] and for comparison with general circulation model simulations to assess model performance [*Soden and Bretherton*, 1994]. A quantitative interpretation of the 6.7-μm measurement is required to successfully incorporate these satellite observations into a description of the upper tropospheric water vapor budget. Recently, *Soden and Bretherton* [1993] described a method of deriving an upper tropospheric relative humidity based upon observations from the GOES 6.7-μm channel. This method is summarized in the next section.

The Raman lidar and CLASS measurements obtained during the FIRE Cirrus-II experiment represent a unique opportunity to verify the GOES upper tropospheric relative humidity measurements by providing state-of-the-art measurements of upper tropospheric water vapor which are independent of the GOES observations. The lidar and CLASS measurements are also valuable for their high vertical resolution in the upper troposphere. This study combines the satellite and independent observations to (1) evaluate the reliability of GOES upper tropospheric humidity observations

[1]Atmospheric and Oceanic Sciences Program, Princeton University, Princeton, New Jersey.
[2]Now at NOAA Geophysical Fluid Dynamics Laboratory, Princeton, New Jersey.
[3]Cooperative Institute for Meteorological Satellite Studies, University of Wisconsin, Madison.
[4]NASA Goddard Space Flight Center, Greenbelt, Maryland.
[5]Hughes STX Corporation, Lanham, Maryland.

Paper number 94JD01721.
0148-0227/94/94JD-01721$05.00

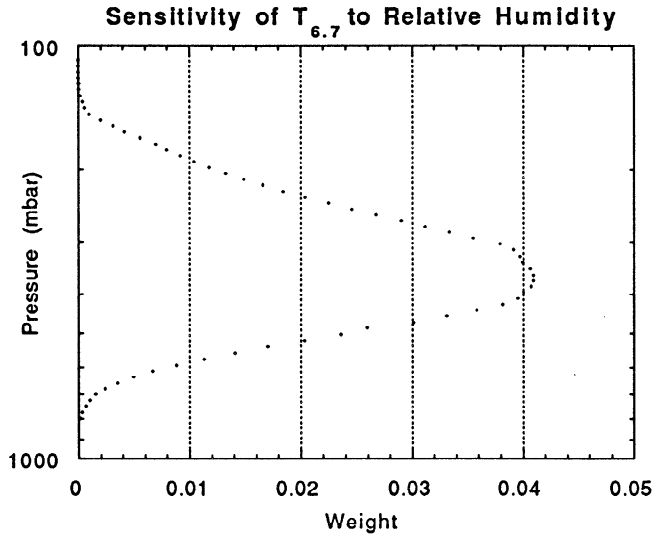

Figure 1. The vertical sensitivity of the 6.7-μm channel to variations in relative humidity. The sum of the weights to individual points is unity.

and (2) examine the impact of vertical variability in the moisture profile upon the GOES upper tropospheric humidity measurements. The next section summarizes the data and analysis procedure used. Section 3 compares the GOES upper tropospheric humidity measurements with simultaneous CLASS and Raman lidar observations. Section 4 examines the effect of vertical variability in relative humidity profile upon the derived product and section 5 summarizes our conclusions.

2. Data and Analysis Procedure

2.1. GOES

Several studies have employed satellite observations in the 6.3-μm water vapor absorption band to describe the distribution of water vapor in the upper troposphere [*Hayden et al.*, 1981; *Schmetz and Turpeinen*, 1988; *Wu et al.*, 1992; *Soden and Bretherton*, 1993]. This paper makes use of 6.7-μm spectral measurements made by the Visible Infrared Spin Scan Radiometer (VISSR) Atmospheric Sounder (VAS) on board GOES 7. The VAS instrument provides 6.7-μm radiances every 30 min with a nadir resolution of approximately 16 km. In-flight calibration of an earlier VAS instrument suggests random noise in individual observations of +/- 0.75 K with possible biases of up to 1.9 K due to calibration uncertainties [*Menzel et al.*, 1981].

Although satellite measurements in the 6.7-μm channel provide a valuable source of information on upper tropospheric water vapor, they have been sorely underutilized for climate studies. One reason for this stems from the difficulty of interpreting brightness temperatures in terms of a more familiar water vapor quantity. *Soden and Bretherton* [1993] addressed this issue by developing an interpretation tool, based upon a simplified model of radiative transfer, which provides a convenient means of interpreting 6.7-μm brightness temperature in terms of an upper tropospheric humidity index (UTH). The UTH corresponds roughly to a vertically averaged relative humidity in a layer from 500 to 200 mbar (or roughly 5.5-12.0 km). A more precise description of the vertical sensitivity of UTH is given in section 4. Using the Goody random band model and assuming strongly-absorbing pressure-broadened lines, *Soden and Bretherton* [1993] demonstrated that for an atmospheric profile corresponding to a constant lapse rate and relative humidity, the 6.7-μm brightness temperature ($T_{6.7}$) varied logarithmically with the ratio of UTH and cosine of the satellite-viewing zenith angle (θ).

$$\log\left(\frac{\mathrm{UTH}}{\cos\theta}\right) = a + bT_{6.7} \qquad (1)$$

The relationship between UTH and $T_{6.7}$ described by equation (1) was determined theoretically based upon a simplified treatment of the radiative transfer at 6.7-μm. In their study, Soden and Bretherton performed detailed calculations of $T_{6.7}$ using the Cooperative Institute for Meteorological Satellite Studies (CIMSS) transmittance model (which includes the GOES 7 spectral response function) and input profiles of temperature and moisture supplied by European Centre for Medium-Range Weather Forecasts (ECMWF) operational analyses for July 1987. The coefficients, a=31.5 and b=-0.115 K^{-1}, were then determined empirically by regressing the simulated $T_{6.7}$ against the corresponding vertically weighted average of the upper tropospheric relative humidity calculated directly from the same ECMWF profiles. In this way, a consistent set of coefficients were derived to relate observed (or simulated) $T_{6.7}$ to UTH. These coefficients were in good agreement with the values expected based upon the theoretical construct of the simplified model. Furthermore, comparison of the simulated $T_{6.7}$ with the corresponding value of UTH calculated directly from the same profiles revealed a relationship in very good agreement with that predicted by equation (1): rms error of roughly 1 K or 8% in terms of UTH. The good agreement and the similarity between the theoretically estimated and empirically determined coefficients support the validity of the simple relationship described by equation (1).

In essence, equation (1) represents a simplification derived from radiative transfer theory and then tuned slightly to ECMWF analyses for July 1987 and the GOES 7 spectral response function. Although these profiles correspond to only a single month of analyses, they do in fact represent a wide range of upper tropospheric conditions [*Soden and Bretherton*, 1994] and consequently the values of the coefficients are insensitive to seasonal variations in the data set used to derive them. This is demonstrated in the first three columns of Table 1 which compare coefficients obtained using ECMWF analyses from January, April, July, and October. The coefficients from all four months vary by less than 3%, indicating that there is little sensitivity to the

Table 1. Seasonal Regression Coefficients From ECMWF Analyses

	a	b	rms (CLASS/ Lidar)	Bias (CLASS/ Lidar)	Corr. (CLASS/ Lidar)
Jan.	31.2	-0.114	8.4/6.2	-6.1/3.0	0.90/0.93
April	32.0	-0.117	9.3/6.9	-6.7/3.3	0.90/0.93
July	31.5	-0.115	8.9/6.4	-6.5/3.2	0.90/0.93
Oct.	30.9	-0.112	9.9/7.3	-7.2/3.5	0.90/0.93

See text for details.

particular set of input profiles used. The GOES 7 satellite was used in both this study and the study by *Soden and Bretherton* [1993]; thus the sensitivity of the coefficients to slight differences in the spectral response function from one satellite to the next are not an issue here. However, we do note that the sensitivity of the coefficients to differing spectral response functions is typically smaller than the seasonal sensitivities shown in Table 1.

Using equation (1) in combination with the coefficients reported by *Soden and Bretherton* [1993] (a=31.5 and b=-0.115 K^{-1}), the UTH is derived over the FIRE Cirrus-II central site for the entire field phase at 1/2-hourly intervals. To compare the satellite observations with the radiosonde and lidar measurements, it is necessary to identify cloud contaminated 6.7-μm measurements. *Soden and Bretherton* [1993] describe a cloud clearance procedure for determining an average clear sky radiance over a region of roughly 2.5° latitude by 2.5° longitude. However, since the independent observations represent point measurements, it is here necessary to retain the highest spatial resolution possible in the satellite data. Consequently, cloud screening is performed by visual inspection of coincident 11-μm (IR window) imagery during the period of study. Since the focus of this report is to compare the GOES observations of upper tropospheric moisture with independent radiosonde and lidar measurements, the development of a cloud clearance algorithm for pixel resolution 6.7-μm data will be the subject of a separate study.

2.2. Raman Lidar

The FIRE Cirrus-II experiment was the first field deployment of a new NASA/GSFC (Goddard Space Flight Center) Raman water vapor lidar system. This lidar, described by *Whiteman et al.* [1992a] and *Ferrare et al.* [1992], incorporated many new features and was significantly improved over the previous system described by *Melfi and Whiteman* [1985], *Melfi et al.* [1989], *Whiteman et al.* [1992b], and *England et al.* [1992]. The characteristics of this new lidar, as operated during the FIRE Cirrus-II experiment, will be discussed here briefly. The system uses a XeF laser to transmit light pulses at 351 nm. A telescope collects the combined aerosol and molecular backscattered light at the laser wavelength as well as Raman scattered light from water vapor (403 nm), nitrogen (383 nm), and oxygen (372 nm) molecules. Beam splitters are used to separate the return signals into low- and high-sensitivity channels; these two channels are employed for each wavelength to measure signals from throughout the troposphere. Photomultiplier tubes detect the backscattered radiation in all channels and provide output signals to photon counters. In normal operation, data from more than 2300 shots are recorded as 1-min profiles with a range resolution of 75 m. The standard errors for these data are computed using Poisson statistics (i.e., the noise is inversely proportional to the square root of the total number of photon counts). In order to enhance the performance at high altitudes, 60 consecutive 1-min profiles were summed together to form hour averages which were used in the comparison. Figure 2 shows the absolute (Figure 2a) and relative (Figure 2b) errors in water vapor mixing ratio as a function of altitude for one-minute (solid line) and one-hour (dashed line) averaging time for typical Spectral Radiative Experiment (SPECTRE) data. The decrease in error for altitudes between 4.0 and 4.5 km corresponds to the

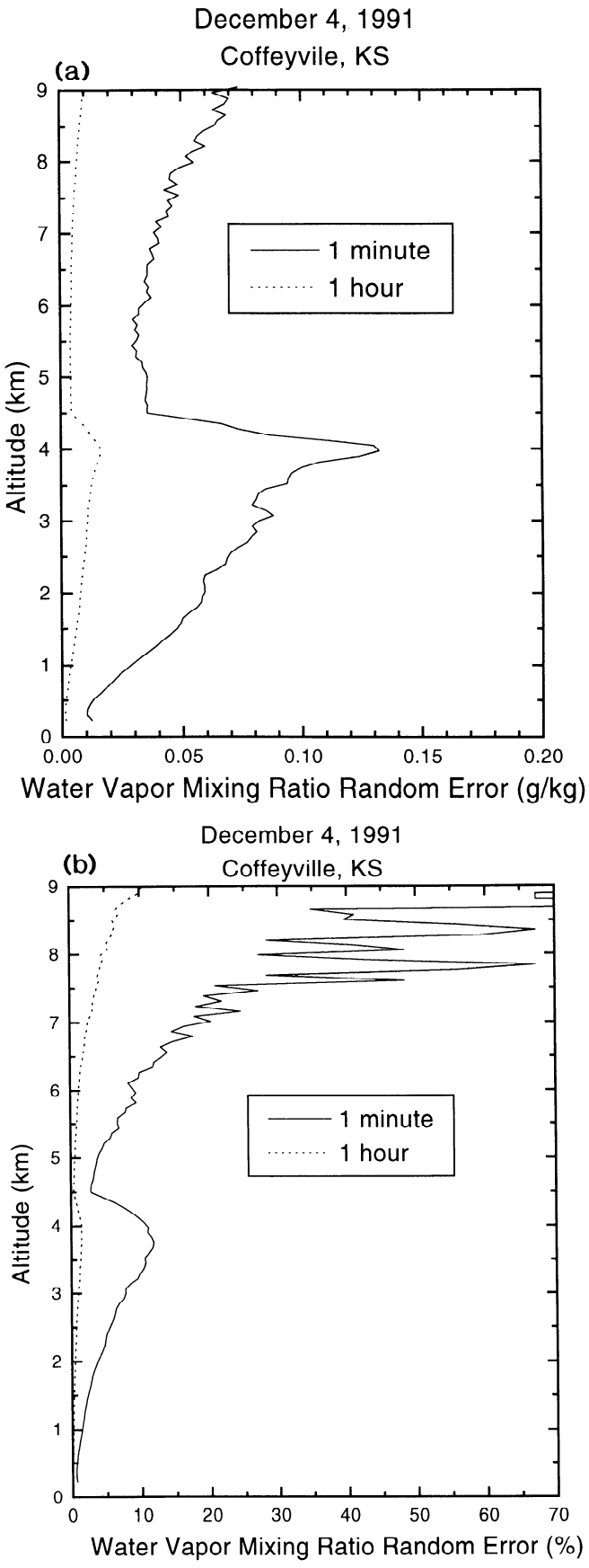

Figure 2. (a) Absolute and (b) relative errors in water vapor mixing ratio as a function of altitude for one-minute (solid line) and one-hour (dashed line) averaging times for typical SPECTRE data.

transition from using low sensitivity channel data (below 4 km) to high sensitivity channel data (above 4.5 km). The one-hour averaging clearly provides a significant reduction in water vapor retrieval errors, particularly in the upper troposphere (see Figure 2b).

Profiles of water vapor mixing ratio are computed from the ratio of the Raman water vapor to Raman nitrogen return signals. A small correction (<7% for altitudes below 12 km) is applied to account for the differential atmospheric transmission between these two Raman wavelengths. To further reduce the noise at high altitudes, the water vapor profiles have been smoothed using a "nearly equal ripple" digital filter [*Kaiser and Reed*, 1977]. This smoothing reduces the vertical resolution from 75 m (below 8 km altitude) to 300 m (between 8 and 10 km). The estimated precision of the smoothed moisture profiles decreases with height, ranging from 0.5% at 500 mbar to 5-7% near 300 mbar. Since the lidar measures backscattered radiation in the visible spectrum, the water vapor retrievals are performed only during nighttime hours resulting in 5 to 10 1-hour integrations per 24-hour period. Furthermore, clouds rapidly attenuate the laser beam so that water vapor retrievals are generally limited to altitudes below cloud base.

The lidar water vapor mixing ratio profiles are calibrated using a weighted least squares regression of the lidar ratios to the water vapor mixing ratios measured by coincident radiosondes launched at the lidar site. Each radiosonde is used independently to derive an altitude-independent calibration coefficient and the average from all coefficients is used in this study. If the relative humidity for a particular level is below 30%, data for that level are not used in the calibration because of potential unreliable radiosonde moisture measurements in dry conditions [*Wade and Wolfe*, 1989; *Garand et al.*, 1992]. However, the calibration is based upon observations at all levels below 8 km. Thus even though the upper tropospheric humidity may have been below 30% for a particular observation, it does not mean that many levels were not used from that profile. If no clouds were present and all radiosonde relative humidities between 0 and 8 km were above 30%, then approximately 100 data points would have been used to determine an individual calibration coefficient. However, on average there were roughly 45 data points due to the cloud and relative humidity restriction. During the 3-week FIRE Cirrus-II experiment period, there were 41 radiosonde humidity profiles used for calibration. Of the 41 profiles, 24 were made by Atmospheric Instrument Research, Inc. (AIR) sondes which use carbon hygristor elements, while 17 were made with CLASS sondes which use capacitive elements. Initial results from these and other comparisons indicate that the lidar water vapor mixing ratio calibration constant derived using the radiosonde capacitive humidity sensor measurements is systematically 5-6% lower than that derived using the carbon hygristor humidity measurements. Since it is not clear which (if either) radiosonde humidity sensor provides the more accurate humidity measurement, the lidar calibration constant was found using data from all 41 comparisons so that, on average, the lidar water vapor mixing ratios lie approximately halfway between those measured by the two radiosonde sensors. All available radiosonde measurements are used in order to obtain the best calibration possible. Since some CLASS sondes are used in the calibration, the lidar measurements are not completely independent of the CLASS measurements. However, both instruments are independent from the GOES data which is the focus of this investigation. Furthermore, the greater reliance of AIR sondes (60%) relative to CLASS sondes (40%) and inclusion of lower tropospheric levels for calibration enhance the independence of the lidar upper tropospheric measurements. If only AIR sondes were used, the lidar humidity measurements would have been roughly 2% higher than the values reported here. In addition, the lidar calibration coefficients are distributed uniformly with time, so that had only a portion of the field experiment been used to calibrate the lidar (enabling the remaining portion to be independent) the calibration would not have differed significantly from the actual value used.

Lidar data above 300 mbar (~ 9.5 km) are not used in the subsequent data analysis because of a problem which is believed to stem from signal-induced noise in the photomultiplier tubes used during this experiment. When present in the high-sensitivity water vapor channel, the noise can produce overestimates of relative humidity at high altitudes where the mixing ratios are small and thus the water vapor signals are weak. Subsequent measurements taken after the FIRE Cirrus-II experiment with different photomultiplier tubes show improved performance in high-altitude water vapor measurements.

2.3. CLASS

In situ measurements of atmospheric profiles of temperature and relative humidity over the FIRE Cirrus-II field site are provided by the Cross-Chain Loran Atmospheric Sounding System (CLASS). The CLASS consists of a model RS80 Vaisala radiosonde equipped with a capacitance moisture sensor and a Loran-C navigation system to determine the sonde trajectory. The temperature and humidity soundings consist of point measurements along the sonde trajectory. The data are smoothed using a 20-s time average yielding profiles with a vertical resolution of roughly 5 mbar. CLASS sondes were launched 5-7 times per day during FIRE Cirrus-II Intensive Observation Periods (IOPs) providing accurate temperature, moisture, and wind information in support of the experiment.

2.4. Comparison Procedure

The GOES observations provide measurements of the relative humidity vertically averaged over a range of pressure in the upper troposphere (roughly 500-200 mbar). The CLASS measurements, on the other hand, yield vertical profiles of temperature and moisture. Therefore to compare GOES UTH with the radiosonde measurements, a two-step "profile-to-satellite" procedure is used. In the first step, CLASS profiles of temperature and moisture are inserted into the CIMSS transmittance model to simulate a $T_{6.7}$ which would be observed by the satellite under those conditions. The second step transforms both the GOES observed $T_{6.7}$ and the CLASS simulated $T_{6.7}$ into UTH quantities using equation (1). Hence the observed and simulated $T_{6.7}$ are treated in a consistent manner. In this way, the use of the empirically derived regression coefficients does not cause spurious differences between the GOES and CLASS UTH because the same coefficients are applied to both the GOES and CLASS $T_{6.7}$. Essentially, it is $T_{6.7}$ which are being compared, only the comparison is being performed in UTH space rather than brightness temperature space to facilitate interpretation of the

results in terms of a more familiar water vapor quantity. This procedure is more accurate than comparing GOES UTH with an explicit vertical average of the relative humidity since it accounts for vertical variations in the moisture profile and the slight temperature dependence of the channel, as well as removing spurious differences between the two data sets which could arise from biases in the empirical coefficients. Hence it provides the accuracy of comparing observed with simulated brightness temperatures as well as an easily interpretable measure of upper tropospheric moisture. An identical procedure was used by *Soden and Bretherton* [1994] to compare GCM profiles of temperature and moisture with GOES observations of $T_{6.7}$.

A similar procedure is used to compare the lidar measurements. Since the lidar provides profiles of moisture only, temperature profiles are interpolated from the nearest radiosonde launches. As mentioned in section 2.2, lidar retrievals above 300 mbar are not used in this study. However moisture profiles up to 100 mbar are needed for the radiative transfer calculations. Therefore to complete the moisture profiles, the relative humidity in the 100 to 300 mbar layer is set equal to the mean relative humidity of the 350 to 300 mbar layer. The precise impact of this filling procedure is difficult to estimate. Inspection of CLASS profiles suggests that relative humidity decreases with height above 300 mbar. Hence, if CLASS profiles are used to estimate the error resulting from the filling procedure, a slight moist bias would be expected. Comparison of the UTH derived from filled CLASS profiles with those obtained from actual CLASS profiles indicates rms differences of approximately 6% with a bias of 3%. However, this bias estimate is strongly dependent upon the accuracy of the CLASS observations from 300 to 100 mbar. Radiosonde measurements in general are suspect at these altitudes due to the low temperatures and resultant small mixing ratios. Indeed, almost all CLASS humidity profiles decrease with height above 300 mbar which could be an indication of reduced sensitivity at high altitudes. Furthermore, water vapor climatologies from SAGE II for 20N-40N [*McCormick and Chiou*, 1994, figures 3 and 4 and table 2], indicate that the relative humidity in the upper troposphere is in fact very nearly constant. Between 300 and 200 mbar (9-11.5 km), typical humidity lapse rates ($dr\!h/dz$) vary from roughly +2%/km to -3%/km depending upon season. For the 200 to 100 mbar layer (11.5-16 km), typical humidity lapse rates are roughly -2.0%/km, although the $T_{6.7}$ is markedly less sensitive to this layer relative to the 300-200 mbar layer (see Figure 1). Using even the largest SAGE humidity lapse rates in place of the constant relative humidity assumption changes the lidar UTH by less than 2%.

3. Intercomparison of UTH Measurements

Time series plots comparing the GOES $T_{6.7}$ (Figures 3a to 3c) and UTH (Figures 3d to 3f) with CLASS and lidar measurements are shown for three different FIRE Cirrus-II IOPs: November 18-22 (Figures 3a and 3d), November 24-26 (Figures 3b and 3e), and December 4-7 (Figures 3c and 3f). These periods provide the densest temporal coverage of CLASS and lidar observations. The UTH for each GOES, CLASS, and lidar data point in Figures 3d to 3f is calculated from the corresponding $T_{6.7}$ in Figure 3a to 3c using equation (1). The GOES measurements are shown by the solid line. Lidar and CLASS observations are denoted by squares and circles, respectively. Observations for times in which the 6.7-μm radiances were contaminated by cloud cover are not shown. The presence of high-frequency variability in the GOES time series is believed to stem primarily from noise in the VAS 6.7-μm sensor [*Soden and Bretherton*, 1993], although natural variability in the UTH field also contributes. The 30-minute fluctuations in $T_{6.7}$ are typically on the order of 1K or roughly 5-10% in terms of UTH and are similar in magnitude to the random instrumental noise in the 6.7-μm channel of 0.75 K reported by *Menzel et al.* [1981] which is ~6% in terms of UTH. Despite the high-frequency variability in the GOES data, analysis of all three periods indicates generally good agreement with both the CLASS and lidar observations. The similarity in the time series of UTH is quite remarkable given the differing spatial characteristics between the GOES and radiosonde/lidar instruments. The extent of the agreement provides confidence in the quantitative use of 6.7-μm satellite measurements to describe the temporal evolution of the upper tropospheric water vapor field over the FIRE Cirrus-II site. The lidar retrievals in particular exhibit good agreement with the GOES data throughout the three IOPs.

Figure 4a shows a scatter plot of the UTH from GOES and lidar measurements. To reduce the impact of instrument noise, the GOES 30-min observations have been smoothed using a 1-2-1 time average centered on the GOES observation nearest the middle of the 1-hour lidar sounding. Temporal averaging is chosen rather than spatial averaging due to an apparent 60-min periodicity in the GOES $T_{6.7}$ noted by *Soden and Bretherton* [1993]. At low to moderate humidities the lidar retrievals tend to be roughly 5% higher than the GOES observations. At higher humidities the bias appears to decrease. The correlation between the GOES and lidar UTH is 0.93 which is significant at the 99% level for 65 degrees of freedom. The rms difference is 6.4%. Thus the GOES and lidar measurements of UTH are consistent to roughly within the estimated uncertainty in either the GOES or lidar retrievals. If the mean bias of 3.2% between the lidar and GOES UTH is removed, the rms difference is reduced to 5.6%. It is worth noting that if the actual lidar profiles rather than the filled profiles are used, both the correlation and bias increase. This suggests that there is a systematic moist bias in the lidar retrievals above 300 mbar but that the observed lidar profiles do correlate well with the presence of moist or dry conditions in the upper troposphere.

For the CLASS observations, the agreement is best during the November 18-22 IOP where differences with the GOES measurements are typically less than 5% UTH. Slightly larger differences resulting from an apparent dry bias in the CLASS relative to the GOES are evident in the subsequent IOPs, although the temporal trends between the GOES and CLASS are still very similar. Despite the systematically lower humidities in the CLASS measurements, the overall agreement between the GOES and CLASS UTH is still quite good as demonstrated in Figure 4b. This figure displays a scatter plot between the UTH derived from both GOES and CLASS measurements. The CLASS UTH are systematically lower than the GOES UTH. The bias increases with increasing UTH from roughly 5% for UTH ~ 15% to 10% for UTH ~ 60%. The correlation between the two observations is 0.90 which is significant at the 99% level for 64 degrees of freedom. The rms difference is 8.9%. When the mean bias of 6.5% is removed, the rms difference between the GOES and CLASS UTH reduces to 6.2%. Table 1 lists the sensitivity of

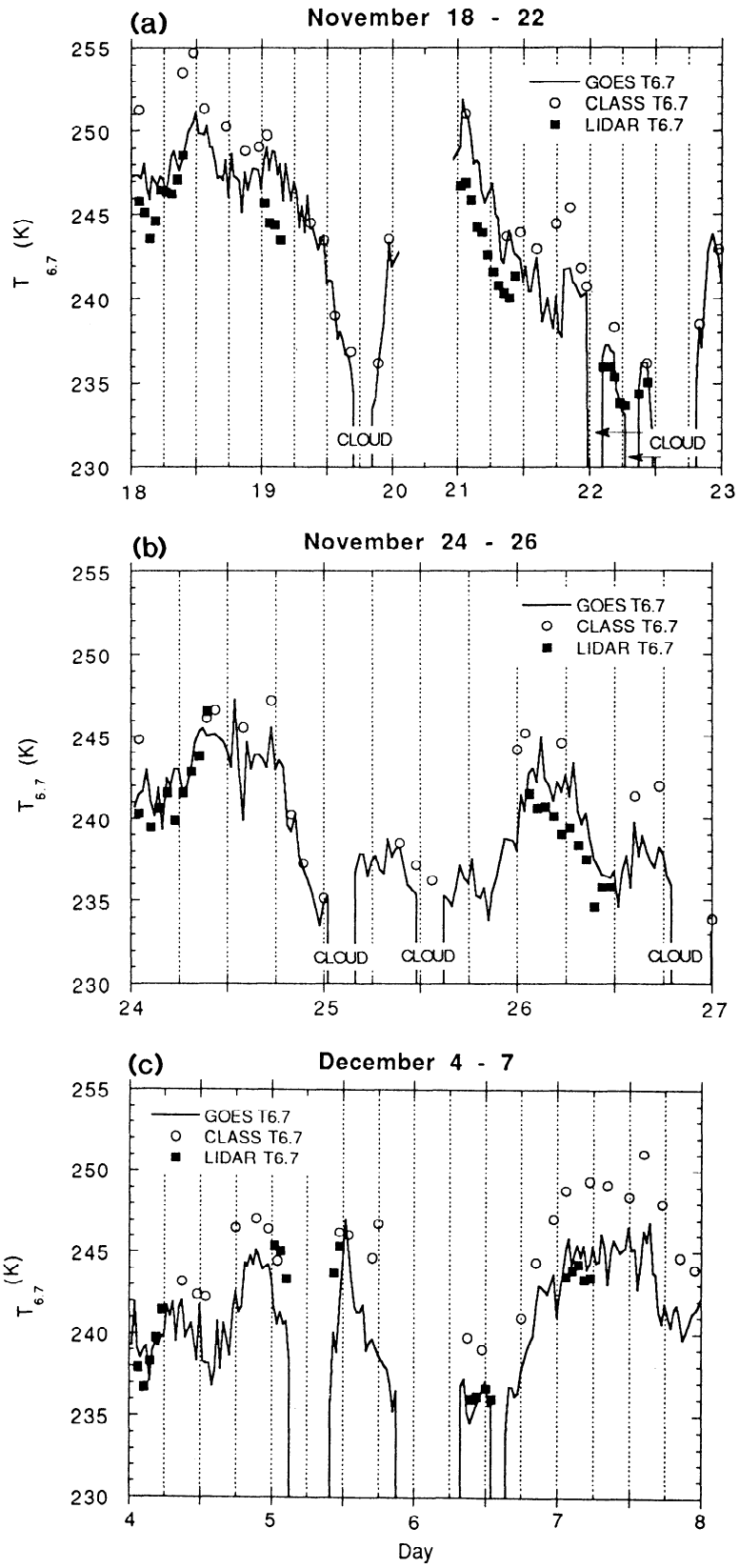

Figure 3. Time series plots of (a-c) $T_{6.7}$ and (d-f) upper tropospheric humidity index (UTH) from GOES (solid line), lidar (squares), and CLASS sondes (circles) for FIRE Cirrus-II Intensive Observation Periods: November 18-22 (Figures 3a and 3e), November 24-26 (Figures 3b and 3d), and December 4-6 (Figures 3c and 3f).

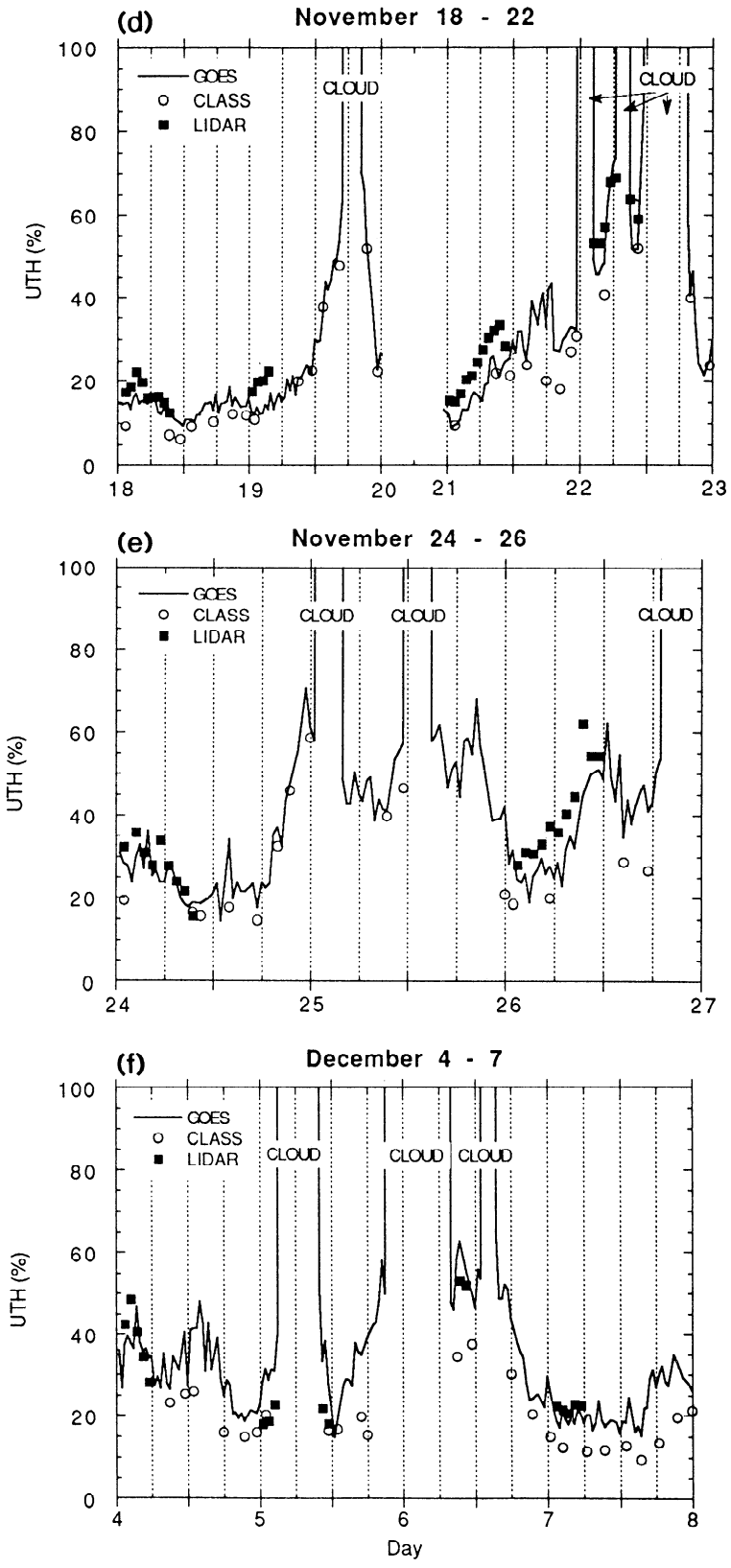

Figure 3. (continued)

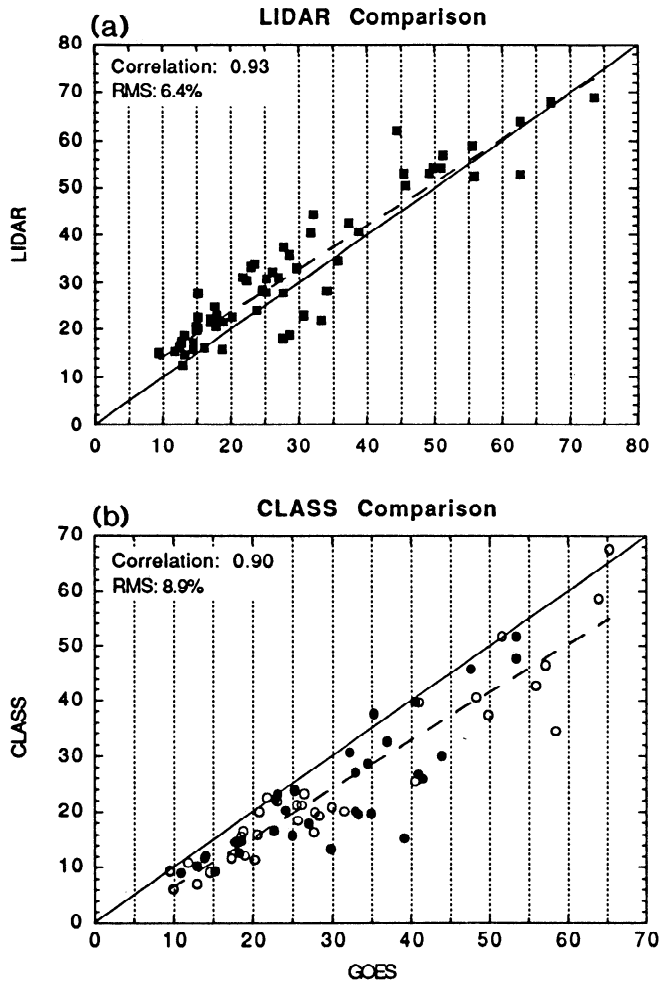

Figure 4. A scatter plot of the upper tropospheric humidity index (UTH) for (a) GOES versus lidar and (b) GOES versus CLASS. The dashed line is a least-squares fit. The solid line is a perfect fit.

the GOES/CLASS and GOES/lidar comparison statistics (bias and rms) to the use of differing seasonal coefficients (*a* and *b*) in equation (1). The correlations are unaffected by the changes in coefficients. The rms and bias values are all very similar, indicating that the differences noted above reflect real discrepancies between the measurements and are not sensitive to the particular set of coefficients used.

Previous studies (*Pratt*, 1985; *Elliot and Gaffen*, 1991) have noted spurious diurnal variations in other radiosonde humidity measurements (i.e. VIZ) due to radiation-induced warming of the interior radiosonde housing. However, the impact of this effect is strongly dependent upon radiosonde design and no systematic analysis has been performed to determine what, if any, radiation-induced errors are present in Vaisala radiosondes (i.e., CLASS). To examine this issue, the data points shown in Figure 4b are separated into day (open circles) and night (solid circles) categories. Table 2 lists statistics calculated separately for each category. The daytime measurements exhibit a larger bias, larger rms difference, and smaller correlation than the nighttime measurements. If the daytime measurements are further stratified into mid-day observations (+/- 2 hours of local noon), the disparity between GOES and CLASS measurements becomes noticeably larger (row 4). These results are consistent with increased errors during daytime hours due to radiative heating, suggesting that the dry bias in CLASS measurements relative to GOES measurements is partially attributable to this effect.

Some of the scatter between the GOES and CLASS measurements may also be attributable to the differing spatial resolutions of the instruments; the GOES pixel is roughly (16 km)^2 whereas the CLASS observations essentially represent point measurements. Consequently, one would expect greater scatter between CLASS and GOES observations in situations of mesoscale water vapor gradients. For example, subpixel variability in humidity may be responsible for the unusually large differences which are evident on December 5, 1700-1800 UT, during which time the CLASS UTH is roughly half as large as the value observed by GOES. Inspection of the GOES time series clearly indicates the passage of a large water vapor gradient over the FIRE Cirrus-II site just prior to this period. Another source of discrepancy could stem from wind drift of the sonde away from the central FIRE site. This may be particularly important in situations of strong vertical shear when the sonde trajectory at lower levels may cause it to cross upper tropospheric streamlines which are typically perpendicular with moisture gradients.

Another noticeable discrepancy occurs on December 6, 0905-1115 UT, where the CLASS UTHs are considerably lower than those observed by GOES. However, near simultaneous lidar measurements are very similar to the GOES values. Comparison of the relative humidity profiles from this time (Figure 5) shows good agreement between the CLASS and lidar measurements up to roughly 350 mbar. Above this level the profiles diverge, with the CLASS relative humidity approaching 5-10%, while the lidar values approach 100%. This pattern of discrepancy between the lidar and CLASS upper tropospheric humidity profiles appears systematically throughout the FIRE Cirrus-II experiment. The discrepancy between the lidar and CLASS values of UTH for the two profiles in Figure 5 is at least partially attributable to the effects of imposing constant relative humidity above 300 mbar (set to the mean for the 350 to 300 mbar layer) for the lidar profiles whereas the CLASS profiles show a strong tendency for decreasing relative humidity with increasing height. However, it is not obvious which is more accurate. As mentioned in section 2, the lidar retrievals have a suspected moist bias at high altitudes. The CLASS observations are also known to contain systematic biases at high altitudes relative to other sensors. For example, *Schmidlin* [1989] noted a dry bias in relative humidity between 500-400 mbar for capacitive (e.g. CLASS) sensors relative to carbon hygristor (e.g. VIZ) sensors ranging from 3-8%. No results were presented for levels above 400 mbar, although it is generally believed that the accuracy of radiosonde measurements degrades with height [*Elliot and Gaffen*, 1991]. This result agrees well with the 5-6% dry bias noted between CLASS and AIR sondes for the FIRE Cirrus-II experiment (section 2.2).

Table 2. Diurnal Statistics for CLASS Versus GOES Comparison

	Bias	rms	Correlation
Night	-5.8	7.8	0.94
Day	-6.6	8.6	0.86
Mid-day	-9.6	10.9	0.84

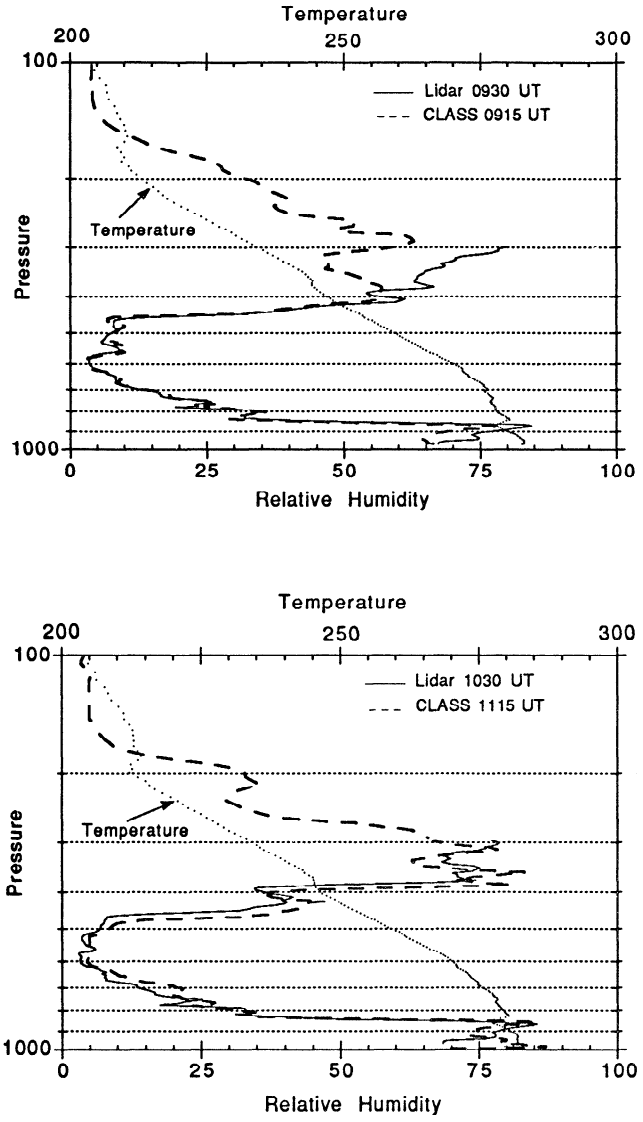

Figure 5. Profiles of relative humidity from lidar (solid) and CLASS sondes (dashed) for December 6, 1991, (top) nearest 0930 UT and (bottom) nearest 1115 UT. Lidar data above 300 mbar are not used in the comparisons with GOES.

Inspection of simultaneous lidar and CLASS profiles from periods when cirrus are present also supports the hypothesis of a dry bias in the CLASS measurements. Figure 6 compares profiles of CLASS relative humidity with the nearest corresponding 1-hour lidar retrieval for December 5 at 0530 and 0930 UT. In both of these profiles, the lidar detects cirrus with a base near 300 mbar and shows increasing relative humidity up to this level where saturation is reached, although the reliability of the humidity profile above cloud base is questionable due to increased cloud contamination. The CLASS relative humidities also increase near the cloud base; however, saturation is never reached. Peak relative humidities in the cloud layer are 50-65% with respect to water or roughly 75-90% with respect to ice. The undersaturation in the cloud layer suggests a dry bias in the CLASS measurements in approximate agreement with that noted by *Schmidlin* [1989], such a bias could explain the systematically lower CLASS UTH estimates relative to the GOES and lidar observations.

Figure 7 depicts histograms of UTH computed from the CLASS (lidar) measurements and from the corresponding subsets of GOES observations which most closely coincide with the CLASS (lidar) observation. Statistics for each distribution are written in the upper right-hand corner. The mean CLASS UTH is roughly 6% lower than the corresponding GOES value. In contrast, the mean lidar UTH is roughly 3% higher than the GOES value. The fact that the GOES measurements are higher than the CLASS observations yet slightly lower than the lidar observations is encouraging, suggesting that the impact of instrumental bias in the 6.7-μm channel upon the derived UTH is smaller than what we are able to resolve given the present uncertainties of the independent observations. Another interesting feature of the histograms is the noticeable positive skew in the distribution, i.e., skew toward larger values. This shape is

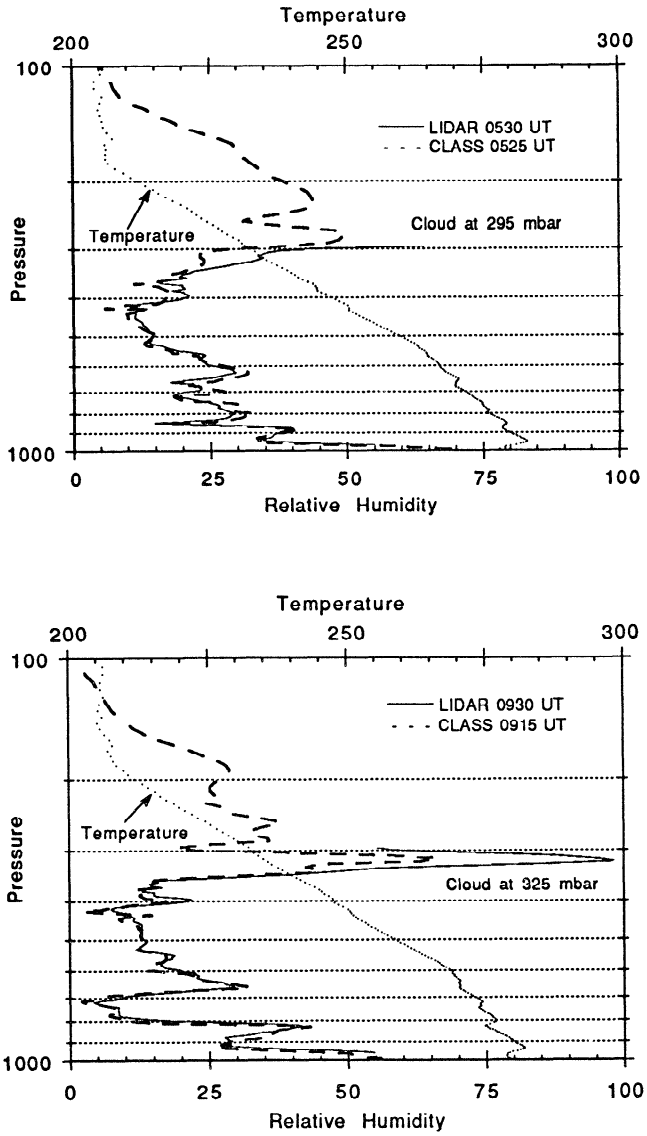

Figure 6. Profiles of relative humidity from lidar (solid) and CLASS sondes (dashed) for sondes launches at (top) 0530 UT and (bottom) 0930 UT. The lidar retrievals are the one-hour averages nearest the CLASS sonde launch. The cloud base pressure is printed in the upper right-hand corner of each profile. Lidar data above 300 mbar are not used in the comparisons with GOES.

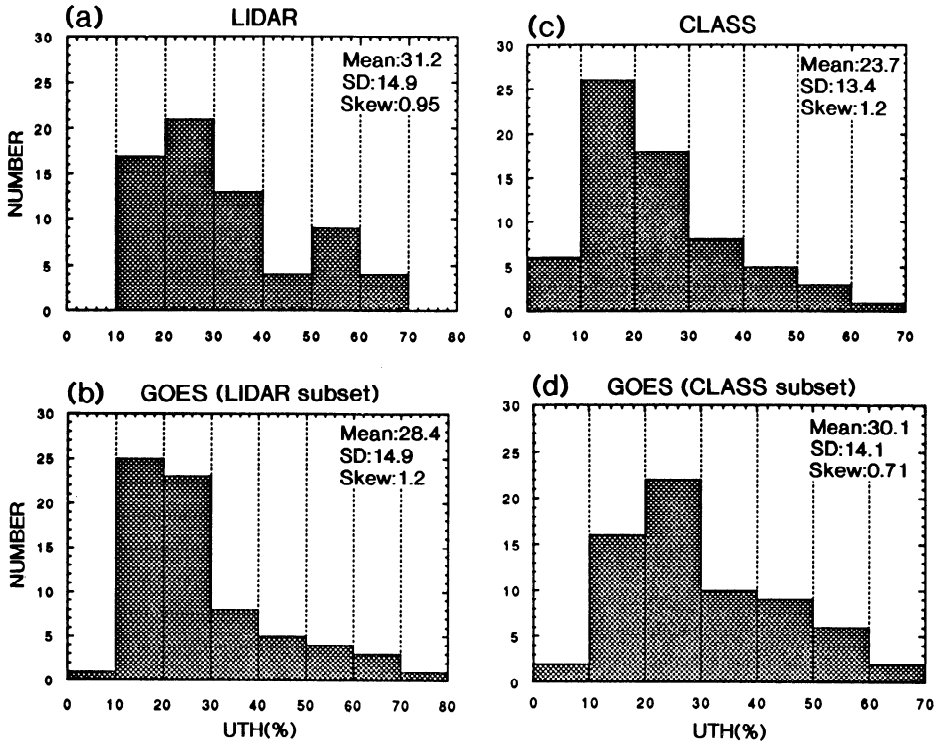

Figure 7. Histograms of the upper tropospheric humidity index (UTH) for (a) lidar, (b) subset of GOES observations which coincide with a lidar observation, (c) CLASS, and (d) subset of GOES observations which coincide with a CLASS observation.

similar to the lognormal distribution noted by *Soden and Bretherton* [1993] for monthly mean UTH. They associated this feature with the exponential decrease in water vapor mass with geometric height combined with a gaussian vertical displacement of parcels along isentropic surfaces. Its presence in histograms of instantaneous measurements from all three instruments attests to the robustness of this feature of the UTH distribution. A more rigorous explanation of this characteristic in terms of isentropic water vapor transport has been proposed by *Pierrehumbert and Yang* [1994].

4. Impact of Vertical Variability on UTH Interpretation

The quantity UTH in equation (1) is defined radiatively. It is the result of transforming an observed brightness temperature based upon a simplified treatment of the radiative transfer at 6.7-μm. For interpretation, however, UTH is to a good approximation equivalent to the vertical average of the relative humidity profile weighted according to the sensitivity of the 6.7-μm channel [*Soden and Bretherton*, 1993]. These weights vary depending upon the moisture and temperature profiles and viewing angle of the satellite. Figure 1 shows the weights for a profile typical of the FIRE site. These weights represent the relative sensitivity of $T_{6.7}$ to perturbations in relative humidity, in thin layers equally spaced in log pressure.

In deriving the expression for UTH in equation (1), Soden and Bretherton assumed a uniform relative humidity throughout the layer to which the 6.7-μm channel is sensitive (roughly 500-200 mbar). The derived UTH corresponds to a vertically-weighted average of this constant relative humidity profile, i.e. the constant value itself. However, inspection of both CLASS and lidar profiles (see Figures 5 and 6) reveals that relative humidity may exhibit significant vertical variability throughout the profile, including the upper troposphere. Therefore it is worth investigating the impact of vertical variability in relative humidity upon the interpretation of UTH using the high-resolution profiles available from the FIRE Cirrus-II experiment. To examine this issue, the values of UTH determined from $T_{6.7}$ calculated using CLASS sonde profiles of temperature and relative humidity are compared to a vertically-averaged relative humidity ($\overline{RH}^{wt}$) using the weights from Figure 1 applied to the corresponding relative humidity profile. The results are shown in Figure 8 as solid circles. The correlation between $\overline{RH}^{wt}$ and UTH is 0.95, and the rms difference is roughly 5% relative humidity. Hence the comparison using high resolution soundings provide further evidence that vertical variability in the humidity profile does not significantly affect the interpretation of UTH from GOES 6.7-μm observations. The requirement of weighting the relative humidity profile according to the sensitivity of the 6.7-μm channel can complicate the interpretation of UTH. Therefore a simpler comparison using the linearly averaged relative humidity between 200 and 500 mbar,

$$\overline{RH}^{lin} = (1/(z_{200} - z_{500})) \int_{z_{500}}^{z_{200}} rh\,dz \qquad (2)$$

is also shown in Figure 8 (open circles). The agreement between UTH and $\overline{RH}^{lin}$ is only slightly worse than with $\overline{RH}^{wt}$: r=0.94, rms=6%. We note, however, that these results are based upon a limited sample of observations from a single geographic location. Thus the vertical variability in these profiles may not be representative of that for all locations.

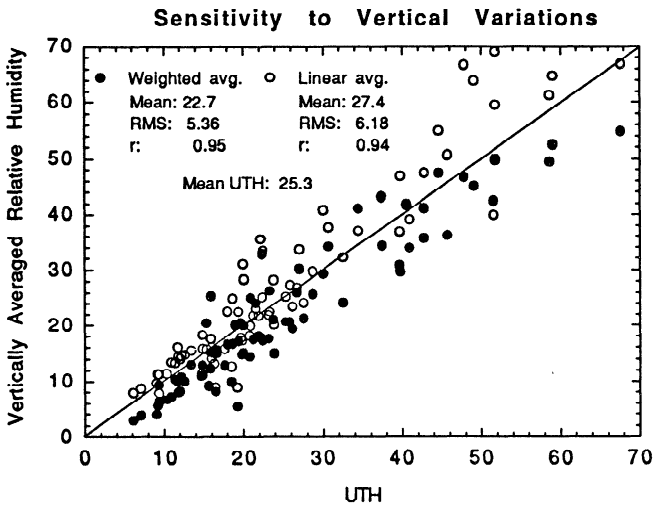

Figure 8. A scatter plot of the upper tropospheric humidity index (UTH) versus $\overline{RH}^{wt}$ (solid circles) and $\overline{RH}^{lin}$ (open circles) based upon calculations from CLASS profiles of temperature and relative humidity

Nevertheless, the results for this region suggest that, to a reasonable approximation, UTH may be interpreted simply as a linear average of the relative humidity profile through the appropriate depth of atmosphere. However, since the depth of atmosphere to which the 6.7-μm channel is sensitive shifts systematically with the temperature and moisture profile and the satellite viewing angle, the comparison of observed $T_{6.7}$ with relative humidity profiles should be accomplished by performing radiative transfer calculations using the temperature and moisture profiles as input. The resulting comparison of calculated and observed $T_{6.7}$ can then be interpreted by transforming both into UTH as was done in section 3.

5. Conclusions

Observations of upper tropospheric relative humidity from the GOES 6.7-μm channel were compared with Raman lidar and CLASS sonde measurements from the FIRE Cirrus-II field experiment. The GOES measurements exhibited very good agreement with both the lidar and CLASS sonde observations. A correlation of 0.93 and an rms difference of 6.4% UTH were noted between the GOES and lidar measurements. A correlation of 0.90 and an rms difference of 8.9% UTH were noted between the GOES and CLASS sonde measurements. The slightly larger differences between the GOES and CLASS measurements stem from a systematic underestimate in the upper tropospheric moisture relative to the GOES observations. This bias is consistent with that noted in a recent radiosonde intercomparison by *Schmidlin* [1989]. A temporal stratification of the CLASS data suggests that the magnitude of this bias is dependent upon time of day and may indicate a solar heating effect on the radiosonde sensor. The good overall agreement between GOES and independent observations of UTH combined with the greater spatial and temporal coverage afforded by satellites encourages the use of 6.7-μm measurements to accurately describe the distribution and temporal evolution of the upper tropospheric water vapor field.

The impact of vertical variability upon the interpretation of the derived UTH was also studied. Comparison of the UTH determined from CLASS profiles of temperature and relative humidity with the corresponding vertically averaged relative humidity indicates that vertical variability in the relative humidity profile does not significantly affect the interpretation of $T_{6.7}$ in terms of UTH. The results suggest that the inferred UTH is typically within about 5% of the relative humidity vertically averaged over the depth of atmosphere to which the 6.7-μm channel is sensitive (500-200 mbar).

Acknowledgements. We wish to thank personnel at GSFC (Dave Whiteman and Keith Evans) and at Sandia National Labs (John Goldsmith, Scott Bisson, and Marshall Lapp) who were responsible for the GSFC Raman lidar data acquisition. We also thank Hal Woolf for assistance with the CIMSS transmittance model, Don Wylie for archiving the GOES data, and Leo Donner, V. Ramaswamy, and two anonymous reviewers for their suggestions.

References

Elliot, W. P. and D. J. Gaffen, On the utility of radiosonde humidity archives for climate studies, *Bull. Am. Meteorol. Soc.*, *72*, 1507-1520, 1991

England, M.N., R.A. Ferrare, S.H. Melfi, and D.N. Whiteman, Atmospheric water vapor measurements: Comparison of microwave radiometry and lidar, *J. Geophys. Res.*, *97*, 899- 916, 1992.

Ferrare, R.A., S.H. Melfi, D.N. Whiteman, and K.D. Evans, Raman lidar measurements of Pinatubo aerosols over southeastern Kansas during November-December 1991, *Geophys. Res. Lett.*, *19*, 1599-1602, 1992.

Garand, L., C. Grassotti, J. Halle, and G. L. Klein, On differences in radiosonde humidity-reporting practices and their implications for numerical weather prediction and remote sensing, *Bull. Am. Meteorol. Soc.*, *73*, 1417-1423, 1992.

Hayden, C. M., W. L. Smith, and H. M. Woolf, Determination of moisture from NOAA polar orbiting satellite sounding radiances, *J. Appl. Meteorol.*, *20*, 450-466, 1981.

Kaiser, J. F. and W. A. Reed, Data smoothing using low-pass digital filters, *Rev. Sci. Instrum.*, *48*, 1447-1457, 1977.

McCormick, M. P. and E. W. Chiou, Climatology of water vapor in the upper troposphere and lower stratosphere determined from SAGE II observations, Paper presented at *5th Symposium on Global Change Studies*, Am. Meteorol. Soc., Nashville, TN, January 6-10, 1994.

Melfi, S.H. and D.N. Whiteman, Observation of lower atmospheric moisture structure and its evolution using a Raman lidar, *Bull. Amer. Meteorol. Soc.*, *66*, 1282-1292, 1985.

Melfi, S.H., D.N. Whiteman, and R. Ferrare, Observation of atmospheric fronts using Raman lidar moisture measurements, *J. Appl. Meteorol.*, *28*, 789-806, 1989.

Menzel, W. P., W. L. Smith, and L. D. Herman, Visible infrared spin-scan radiometer atmospheric sounder radiometric calibration: An in-flight evaluation from intercomparison with HIRS and radiosonde measurements, *Appl. Opt.*, *15*, 358-363, 1981.

Pierrehumbert, R. T. and H. Yang, Production of dry air by isentropic mixing, *J. Atmos. Sci.*, in press, 1994.

Pratt, R. W., Review of radiosonde humidity and temperature errors, *J. Atmos. and Oceanic Tech.*, 2, 404-407, 1985.

Schmetz, J and O. M. Turpeinen, Estimation of upper tropospheric relative humidity file from METEOSAT water vapor image data, *J. Clim. Appl. Meteorol.*, *27*, 889-899, 1988.

Schmidlin, F. J., *WMO International radiosonde intercomparison,*

phase II, final report, 113 pp., World Meteorol. Organ., Geneva, Switzerland, 1989.

Soden, B. J. and F. P. Bretherton, Upper tropospheric relative humidity from the GOES 6.7-μm channel: Method and climatology for July 1987, *J. Geophys. Res.*, *98*, 16669-16688, 1993.

Soden, B. J. and F. P. Bretherton, Evaluation of the water vapor distribution in general circulation models using satellite observations, *J. Geophys. Res.*, *99*, 1187-1210, 1994.

Starr, D. O'C., and S. H. Melfi, The role of water vapor in climate: A strategic research plan for the GEWEX Water Vapor Project (GVaP). *NASA Conf. Publ. CP-3120*, 50 pp., 1991. (Available from International GEWEX Project Office, Washington, D.C.).

Van de Berg, L., A. Pyomjamsri, and J. Schmetz, Monthly mean upper tropospheric humidities in cloud free areas from METEOSAT observations, *Int. J. Clim.*, *11*, 819-826. 1991.

Wade, Charles G. and Daniel E. Wolfe, Performance of the VIZ carbon hygristor in a dry environment, paper presented at *12th Conference on Weather Analysis and Forecasting*, Am. Meteorol. Soc., Monterey, Calif., October 16-20, 1989.

Whiteman, D. N., S. H. Melfi, R. A. Ferrare, K. A. Evans, L. Ramos-Izquierdo, O.G. Staley, R. D. Di Silvestre, I. Gorin, K. R. Kirks, W. A. Mamakos, L. S. Wan, N. W. Walsh, R. L. Aldridge, Advanced raman water vapor lidar, *16th International Laser Radar Conference, NASA Conf. Publ. 3158, part 2*, 483 - 484, 1992a.

Whiteman, D. N., S. H. Melfi, and R. A. Ferrare, Raman lidar system for the measurement of water vapor and aerosols in the earth's atmosphere, *Appl. Opt.*, *31*, 3068-3082, 1992b.

Wu, X., J. J. Bates, and S. J. S. Khalsa, A climatology of the water vapor band brightness temperatures from NOAA operational satellites, *J. Clim.*, *6*, 1282-1300, 1992.

S. A. Ackerman, Cooperative Institute for Meteorological Satellite Studies, University of Wisconsin, Madison, WI 53706. (e-mail:stevea@ssec.wisc.edu)

R. A. Ferrare, Hughes STX Corporation, Lanham, MD 20706. (e-mail: ferrare@mv5.dnet.nasa.gov)

S. H. Melfi and D. O'C. Starr, NASA Goddard Space Flight Center, Greenbelt, MD 20771 (e-mail: melfi@climate.gsfc.nasa.gov : starr@climate.gsfc. nasa.gov)

B. J. Soden, NOAA/Geophysical Fluid Dynamics Laboratory, P.O. Box 308, Princeton University, Princeton, NJ 08540. (e-mail: bjs@gfdl.gov)

(Received November 15, 1993; revised May 4, 1994;
accepted June 27, 1994.)